Dissecting the Membrane Binding and Insertion Kinetics of a pHLIP Peptide[†]

Jia Tang and Feng Gai*

Department of Chemistry, University of Pennsylvania, Philadelphia, Pennsylvania 19104

Received June 11, 2008

ABSTRACT: When it is bound to lipid bilayers, the conformation and location of the membrane pH (low) insertion peptide (pHLIP) depend on pH. This unique feature allows us to explicitly measure the kinetics leading to different membrane-bound states of pHLIP using a model membrane and stopped-flow technique. Our results show that the membrane association kinetics of pHLIP are multiexponential and are consistent with a parallel membrane interaction mechanism. Interestingly, our results also show that the overall rate at which the membrane-inserted state is formed is almost identical to that of formation of the surface-bound state, while prebinding slows the rate of peptide insertion.

Engelman and co-workers have recently shown that the membrane pH (low) insertion peptide (pHLIP) constitutes an attractive model system for studying the mechanism of membrane protein folding and insertion, among other applications (*1*–*5*). This is due to the unique properties of pHLIP. (a) It is soluble and unstructured in aqueous solution near neutral pH. (b) It binds to the surface of lipid membranes near neutral pH as an extended chain (hereafter called the surface-bound state). (c) It inserts into lipid membranes to form a transmembrane α-helix (hereafter called the membrane-inserted state) at low pH when the aspartic acid residues (Asp) in the sequence are protonated. (d) Unlike antimicrobial peptides, it remains monomeric when bound to membranes and thus does not induce membrane fusion or damage (*4*). While the thermodynamic aspects of pHLIP−membrane interactions have been extensively studied (*1, 4, 5*), little is known about the kinetics and hence the mechanism governing pHLIP−membrane association. Herein, we report the kinetics of binding and insertion of pHLIP to a model membrane, POPC (1-palmitoyl-2-oleoyl-*sn*-glycero-3-phosphocholine), under different conditions.

The pHLIP studied here has the sequence GGEQNPIYWARYADWLFTTPLLLLDLALLVDADEGT, which was synthesized using standard Fmoc-based solid-phase synthesis protocols employing a double-coupling strategy. As shown (Figure 1), upon association of pHLIP with POPC vesicles (*6*), its tryptophan (Trp) fluorescence increases. However, compared to that obtained at pH 8.0, the increase at pH 4.0 is considerably larger. This is consistent with the study of Reshetnyak et al. (*4*), which shows that upon formation of the surface-bound state (e.g., at pH 8.0) only one Trp residue changes its environment, whereas in the membrane-inserted state both Trp residues are buried in the hydrophobic region of the membrane. Thus, this pH-dependent change in Trp fluorescence makes it feasible to measure the kinetics leading to different membrane-bound states of pHLIP. Below we discuss such kinetics measured with a home-built stopped-flow apparatus (*7, 8*).

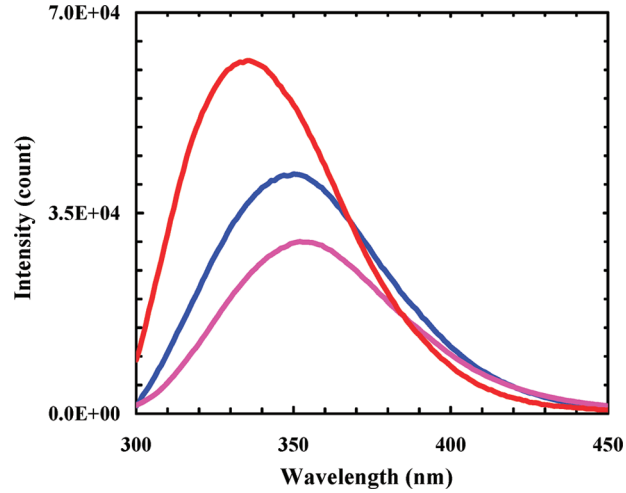

FIGURE 1: Fluorescence spectra of pHLIP (2 μM) in its solution state (magenta) [10 mM phosphate buffer (pH 8.0)], surface-bound state (blue) [1 mM POPC vesicle (pH 8.0)], and membrane-inserted state (red) [1 mM POPC vesicle (pH 4.0)]. These data were collected at 20 °C with a λ_{ex} of 290 nm.

First, we measured the kinetics of association of pHLIP to POPC vesicles at pH 8.0, which lead to the formation of the surface-bound state. As shown (magenta line in Figure 2), the Trp fluorescence increases as a function of time, consistent with the equilibrium measurement (Figure 1). Interestingly, the corresponding stopped-flow kinetics require a minimum of three exponentials to fit (see below). Since in the surface-bound state pHLIP is only peripherally bound to the vesicles and does not oligomerize under the current condition (*4*), these results suggest that the process of binding of pHLIP to POPC vesicles near neutral pH either involves intermediate states or yields two distinguishable (by the current approach) surface-bound conformational ensembles (see below).

Second, we investigated the kinetics of association of pHLIP with POPC vesicles at pH 4.0, which lead to the formation of the membrane-inserted state. As shown (red line in Figure 2), the overall increase in the Trp fluorescence is clearly larger than that obtained in the first experiment, consistent with the equilibrium results (Figure 1). In addition, the corresponding stopped-flow kinetics also follow a nonexponential time course that can be described by a three-exponential function. Surprisingly, the rate constants recovered from the fitting are almost identical to those obtained in the first experiment. In fact, the stopped-flow kinetics

[†] We gratefully acknowledge financial support from the NIH (Grants GM-065978 and RR-01348).

10.1021/bi801103x CCC: $40.75
Published on Web 07/18/2008

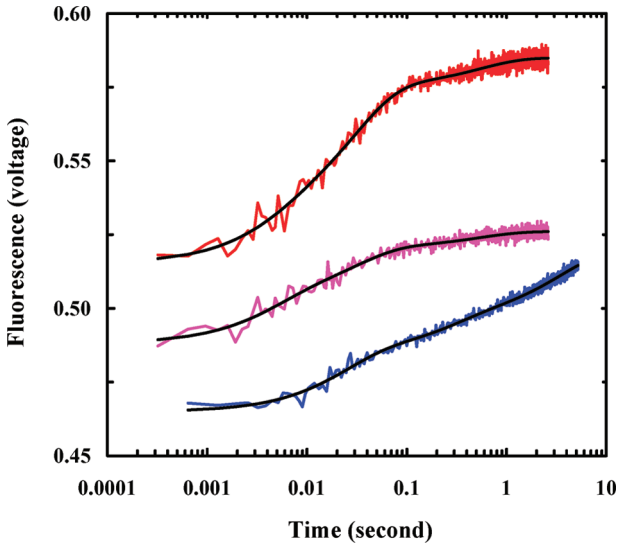

FIGURE 2: Stopped-flow kinetics obtained at 20 °C and under different mixing conditions. For the trace colored magenta, the process was initiated by mixing equal volumes of pHLIP in 10 mM phosphate buffer (pH 8.0) with POPC vesicles (pH 8.0). For the trace colored red, the process was initiated by mixing equal volumes of pHLIP in 10 mM phosphate buffer (pH 8.0), POPC vesicles (pH 8.0), and a HCl solution (pH 1.6). For the trace colored blue, the process was initiated via a pH jump from 8.0 to 4.0 by mixing equal volumes of a pre-equilibrated peptide/vesicle solution (pH 8.0) with a HCl solution (pH 1.9). In all cases, the final peptide and vesicle concentrations were 2 μM and 1 mM, respectively. The Trp fluorescence was excited at 290 nm and collected through a 315 nm long path filter. Smooth lines are fits to a three-exponential function with those kinetic parameters discussed in the text. These data have been offset for clarity.

measured in both cases can be fit globally with the following global rate constants and local relative amplitudes (% at pH 8.0, % at pH 4.0): 231 ± 21 s^{-1} (39%, 21%), 33 ± 4 s^{-1} (46%, 64%), and 1.9 ± 0.4 s^{-1} (15%, 15%). In accordance with previous kinetic studies on other membrane peptides (*7–10*), we assign the first or fastest kinetic phase to the initial bimolecular association of pHLIP with POPC vesicles. By assuming that the initial binding phase occurs under pseudo-first-order conditions and is irreversible, the corresponding second-order binding rate constant is calculated to be 2.3 × 10^5 M^{-1} s^{-1}, which is comparable to that determined for other peptides (*7–10*).

However, interpreting the other two kinetic phases is more difficult since complex kinetics could arise from either a sequential binding−insertion mechanism involving multiple intermediates or a parallel mechanism involving multiple routes. Tentatively, we invoke the following parallel kinetic schemes to describe the stopped-flow kinetics: where P and

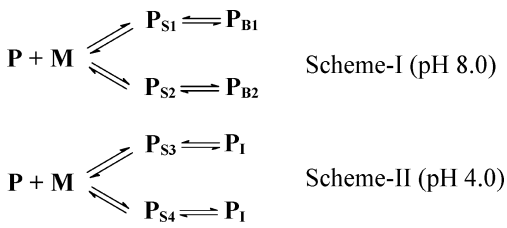

M stand for pHLIP and POPC vesicles, respectively, and subscripts S, B, and I denote the surface-adsorbed, surface-bound, and membrane-inserted pHLIP molecules, respectively. The number denotes a specific conformational ensemble. These parallel schemes suggest that upon initial binding of pHLIP to POPC vesicles two superficially adsorbed conformational ensembles are generated, which can be further stabilized on the membrane surface to reach a surface-bound state or insert into the membrane to reach the membrane-inserted state, depending on the pH. The strongest evidence in support of such a parallel mechanism comes from the fact that in both kinetic traces the second kinetic phase exhibits the largest amplitude. This is inconsistent with a sequential mechanism, at least in the low-pH case, wherein one would expect the largest fluorescence signal to arise from the slowest (or insertion) kinetic step, during which pHLIP is inserted across the lipid bilayer to form a monomeric, transmembrane α-helix (*4, 5*). In addition, Scheme-I is also consistent with previous equilibrium studies indicating that the surface-bound pHLIP is dynamic and hence might sample multiple conformations (*5*). While Trp fluorescence has its limit in differentiating different conformational states, our kinetic results nevertheless suggest that at least two distinguishable surface-bound pHLIP conformational ensembles are populated. These ensembles, which may exhibit different degrees of peptide backbone burial, would show different insertion kinetics in response to protonation of the Asp residues. This is exactly what we have observed in the third experiment (see below). In addition, the apparent peptide insertion rate constants (i.e., 33 ± 4 and 1.9 ± 0.4 s^{-1}) recovered in the current case are also similar to those (in the range of 0.3−30 s^{-1}) obtained for other membrane peptides (*7, 8, 11, 12*).

Interaction with POPC vesicles at pH 4.0 ultimately leads to the insertion of pHLIP into the lipid bilayer as a transmembrane α-helix, whereas at neutral pH, only a portion of the unstructured peptide chain is expected to be buried in the hydrophobic region of the membrane (*1, 4*). Thus, it came as a surprise when at both pH 4.0 and 8.0 the stopped-flow kinetics evolve with almost identical rates. While further studies are required to achieve a microscopic understanding of the factors that control the membrane binding and insertion kinetics of pHLIP, these results nonetheless suggest that the free energy barrier for membrane insertion may arise from burying only a few key residues. Furthermore, these results also suggest that the coil-to-helix transition is not the rate-limiting step for insertion, as observed for antimicrobial peptides (*7, 8*). Interestingly, the rate of insertion of pHLIP into POPC vesicles is much faster than the rate of insertion of a synthetic alanine-rich peptide into DOPC vesicles (*13*), further indicating that the peptide sequence as well as the lipid composition may play a critical role in the kinetics of insertion.

Third, we measured the membrane insertion kinetics of pHLIP directly from its surface-bound state following a pH jump from 8.0 to 4.0, i.e., by mixing a preequilibrated pHLIP/POPC solution at pH 8.0, which is equivalent to the "product" in the first experiment, with a HCl solution of the desired pH. As shown (blue line in Figure 2), the resultant stopped-flow kinetics are quite different from those obtained in the second experiment, although in both cases the final products are essentially the same. In particular, the increase in Trp fluorescence does not reach its maximum even at 5 s, the longest time that can be reached by the current stopped-flow setup, indicating that overall it takes a longer time for pHLIP molecules in the surface-bound state to insert into

POPC membranes in comparison with the insertion rates obtained in the second experiment. It has been shown that it is the protonation of two key aspartic acid residues (i.e., Asp14 and Asp25 in the current peptide sequence) that controls the membrane insertion of pHLIP (*1, 4, 5*). Hence, it is conceivable that the slower insertion rates in this case arise from slow protonation of these residues. If in the surface-bound state one or both of these Asp residues are located beneath the polar headgroup region of the lipids (*14*), one would expect the corresponding protonation rate to become significantly slower than that of protonating solvent-exposed carboxylates. The latter typically occurs with a bimolecular rate constant of approximately 10^{10} M^{-1} s^{-1} (*15*), or on a submillisecond time scale for our case.

Similarly, the kinetic data obtained in the third experiment can be described by a three-exponential function with the following rate constants and relative amplitudes (in parentheses): 43 s^{-1} (36%), 3.8 s^{-1} (21%), and 0.3 s^{-1} (43%). While the slowest rate constant is not accurately determined due to the incomplete stopped-flow kinetics, these results are still in good agreement with an earlier pH-jump experiment in which 70% of the fluorescence signal arising from the insertion of pHLIP from its surface-bound state into DMPC bilayers was observed to occur in approximately 3 s (*1*). Moreover, the three-exponential fitting further indicates that in the surface-bound state pHLIP molecules sample multiple conformational ensembles which exhibit different rates of membrane insertion. Thus, this observation not only corroborates the aforementioned parallel mechanism but also coincides with previous findings that the surface-bound pHLIP is disordered and that the interaction of pHLIP with the bilayer surface distorts the lipids (*4, 5*). More importantly, these results also suggest that the surface-bound species formed at pH 8.0 are different from those (i.e., P_{S3} and P_{S4}) in Scheme-II (pH 4.0).

In summary, we have studied the membrane association kinetics of pHLIP under different conditions in an attempt to provide new insights into the mechanism of pHLIP−membrane interactions. Specifically, we have carried out three experiments to measure the kinetics of association of pHLIP with POPC vesicles from its aqueous phase at pH 8.0 and 4.0 as well as the membrane insertion kinetics from its surface-bound state. Our results show that the membrane association kinetics of pHLIP require multiple exponentials to describe and support a kinetic model for membrane interaction in which the initial binding bifurcates to generate two fluorescently distinguishable surface-adsorbed pHLIP ensembles. Depending on the pH value, these ensembles can either insert into the lipid bilayer to form monomeric transmembrane α-helices or become further stabilized on the membrane surface. Surprisingly, the kinetics leading to these different membrane-bound states of pHLIP are almost identical, suggestive of a local origin for the free energy barrier for peptide membrane insertion. Moreover, our results show that when starting from the surface-bound state, the membrane insertion kinetics of pHLIP not only are heterogeneous but also become slower, suggesting that one or two of the key Asp residues may be sequestered in an environment which has limited accessibility to protons. Taken together, these results provide new insight into the interactions of pHLIP with lipid bilayers. In light of the unique properties of pHLIP and also the interesting findings from this study, it would be desirable to carry out further experimental and computational studies (*16–18*) to substantiate the proposed kinetic mechanisms.

REFERENCES

1. Hunt, J. F., Rath, P., Rothschild, K. J., and Engelman, D. M. (1997) Spontaneous, pH-dependent membrane insertion of a transbilayer α helix. *Biochemistry 36*, 15177–15192.
2. Reshetnyak, Y. K., Andreev, O. A., Lehnert, U., and Engelman, D. M. (2006) Translocation of molecules into cells by pH-dependent insertion of a transmembrane helix. *Proc. Natl. Acad. Sci. U.S.A. 103*, 6460–6465.
3. Andreev, O. A., Dupuy, A. D., Segala, M., Sandugu, S., Serra, D. A., Chichester, C. O., Engelman, D. M., and Reshetnyak, Y. K. (2007) Mechanism and uses of a membrane peptide that targets tumors and other acidic tissues *in vivo*. *Proc. Natl. Acad. Sci. U.S.A. 104*, 7893–7898.
4. Reshetnyak, Y. K., Segala, M., Andreev, O. A., and Engelman, D. M. (2007) A monomeric membrane peptide that lives in three worlds: In solution, attached to, and inserted across lipid bilayers. *Biophys. J. 93*, 2363–2372.
5. Zoonens, M. A., Reshetnyak, Y. K., and Engelman, D. M. (2008) Bilayer interactions of pHLIP, a peptide that can deliver drugs and target tumors. *Biophys. J. 95*, 225–235.
6. POPC (purchased from Avanti Polar Lipids) vesicles (200 nm) were prepared using an extrusion method, the details of which are described in ref *8*.
7. Tucker, M. J., Tang, J., and Gai, F. (2006) Probing the kinetics of membrane-mediated helix folding. *J. Phys. Chem. B 110*, 8105–8109.
8. Tang, J., Signarvic, R. S., DeGrado, W. F., and Gai, F. (2007) Role of helix nucleation in the kinetics of binding of mastoparan X to phospholipid bilayers. *Biochemistry 46*, 13856–13863.
9. Polozov, I. V., Polozova, A. I., Mishra, V. K., Anantharamaiah, G. M., Segrest, J. P., and Epand, R. M. (1998) Studies of kinetics and equilibrium membrane binding of class A and class L model amphipathic peptides. *Biochim. Biophys. Acta 1368*, 343–354.
10. Yandek, L. E., Pokorny, A., and Almeida, P. F. F. (2008) Small changes in the primary structure of transportan 10 alter the thermodynamics and kinetics of its interaction with phospholipid vesicles. *Biochemistry 47*, 3051–3060.
11. Golding, C., Senior, S., Wilson, M. T., and O'Shea, P. (1996) Time resolution of binding and membrane insertion of a mitochondrial signal peptide: Correlation with structural changes and evidence for cooperativity. *Biochemistry 35*, 10931–10937.
12. Constantinescu, I., and Lafleur, M. (2004) Influence of the lipid composition on the kinetics of concerted insertion and folding of melittin in bilayers. *Biochim. Biophys. Acta 1676*, 26–37.
13. Meijberg, W., and Booth, P. J. (2002) The activation energy for insertion of transmembrane α-helices is dependent on membrane composition. *J. Mol. Biol. 319*, 839–853.
14. Tucker, M. J., Getahun, Z., Nanda, V., DeGrado, W. F., and Gai, F. (2004) A new method for determining the local environment and orientation of individual side chains of membrane-binding peptides. *J. Am. Chem. Soc. 126*, 5078–5079.
15. Abbruzzetti, S., Crema, E., Masino, L., Vecli, A., Viappiani, C., Small, J. R., Libertini, L. J., and Small, E. W. (2000) Fast events in protein folding: Structural volume changes accompanying the early events in the N→I transition of apomyoglobin induced by ultrafast pH jump. *Biophys. J. 78*, 405–415.
16. Tieleman, D. P., Berendsen, H. J. C., and Sansom, M. S. P. (2001) Voltage-dependent insertion of alamethicin at phospholipid/water and octane/water interfaces. *Biophys. J. 80*, 331–346.
17. Im, W., and Brooks, C. L. (2005) Interfacial folding and membrane insertion of designed peptides studied by molecular dynamics simulations. *Proc. Natl. Acad. Sci. U.S.A. 102*, 6771–6776.
18. Herce, H. D., and Garcia, A. E. (2007) Molecular dynamics simulations suggest a mechanism for translocation of the HIV-1 TAT peptide across lipid membranes. *Proc. Natl. Acad. Sci. U.S.A. 104*, 20805–20810.

BI801103X